Solar Phys (2013) 284:427–438
DOI 10.1007/s11207-012-0190-7

SDO Observations of Solar Jets

S.P. Moschou · K. Tsinganos · A. Vourlidas · V. Archontis

Received: 24 February 2012 / Accepted: 22 October 2012 / Published online: 21 November 2012

Abstract We present an analysis of high cadence observations of solar jets observed in the Extreme Ultraviolet (EUV), at 304 Å, with the *Atmospheric Imaging Assembly* instrument aboard the *Solar Dynamics Observatory* (SDO). The jets in our sample lie very close to the solar limb to minimize projection effects. Two of the events show clear helical patterns during ejection. We also find that some of the jets are recurrent and that most of them cannot overcome solar gravity.

We investigate the temporal evolution of the jets by measuring the height of their leading edge as a function of time. By fitting the resulting height–time diagrams, we derive the magnitude of their initial ejection speed and plasma acceleration by assuming ballistic motion. Moreover, we calculate the upward acceleration of the jets based on the dynamical velocity of the plasma, without assuming a ballistic motion. In both models, the acceleration profiles suggest the influence of forces other than gravity. In particular, we find indications of an upwards driving force which weakens the decelerating effect of the solar gravitational field

Advances in European Solar Physics
Guest Editors: Valery M. Nakariakov, Manolis K. Georgoulis, and Stefaan Poedts

S.P. Moschou · K. Tsinganos (✉) · V. Archontis
Section of Astrophysics, Astronomy and Mechanics, Department of Physics, University of Athens, Panepistimiopolis 157 84, Zografos, Greece
e-mail: tsingan@phys.uoa.gr

S.P. Moschou
e-mail: sofia_paraskevi@hotmail.com

K. Tsinganos
National Observatory of Athens, Lofos Nymphon, Thissio, Athens, Greece

A. Vourlidas
Space Sciences Division, Naval Research Laboratory, Washington, DC 20375, USA
e-mail: angelos.vourlidas@nrl.navy.mil

V. Archontis
School of Mathematics and Statistics, St. Andrews University, St. Andrews, KY16 9SS, UK
e-mail: vasilis@mcs.st-and.ac.uk

along the motion of the jet. This force is larger in the dynamical model, which indicates that the ballistic approximation does not properly determine the rising motion of the plasma jets.

Keywords Solar jets · Magnetohydrodynamics · Magnetic field · Active regions

1. Introduction

Solar jets are our closest representatives of the broad class of astrophysical jets. Hence, they can be studied with the highest spatial and temporal resolutions. Exploring their nature may help in understanding the physics of their larger astrophysical counterparts (Tsinganos, Ray, and Stute, 2009; Massi and Poletto, 2011).

Various types of solar jet, or more generally, transient collimated brightenings, have been discovered as the wavelength range and the temporal/spatial resolution of solar observations have been improved over the years. Jets, spicules (Beckers, 1972) and surges (Roy, 1973) in Hα, EUV and X-ray jets (Shibata *et al.*, 2007) are among the most common types of plasma flow observed in the low solar atmosphere. Recent solar missions (*e.g.* STEREO, *Hinode*, SDO) and high-resolution ground-based observations (*e.g.* DOT) have provided a detailed picture of such jets over a broad range of spatial and temporal scales throughout the solar atmosphere (Tziotziou, Tsiropoula, and Sütterlin, 2005; Patsourakos *et al.*, 2008; Nisticó *et al.*, 2009).

In many cases, solar jets are associated with bright points caused by episodes of magnetic flux emergence in active regions. Flare-like bright points are transients and likely due to reconnection. Small-scale emerging flux shows up as a bright point, which is not flare-like, but its brightness varies slower. Some jets show structure which suggests a helical magnetic field configuration along the jet (Patsourakos *et al.*, 2008; Liu *et al.*, 2009, 2011; Chen, Zhang, and Ma, 2012; Shen *et al.*, 2011), which might account for the observation of untwisting motions. Coronal jets are also observed inside polar coronal holes, where the plasma beams can be easily seen in emission against the dark background and are not obscured by bright ambient coronal structures (Nisticó *et al.*, 2009). *Hinode* has provided important data on polar jet parameters like duration, size and speed (Kamio *et al.*, 2007; Savcheva *et al.*, 2007; Filippov, Golub, and Koutchmy, 2009) and revealed that the solar chromosphere is full of small-scale jets, which may contribute to the driving of chromospheric and coronal heating. Other studies (Nisticó *et al.*, 2009) suggest that jets may also contribute to the mass flow ejected by the Sun in the form of the solar wind.

The most well-studied jets are those observed in X-rays. A statistical study of about 100 X-ray jets observed with the *Soft X-ray Telescope* (SXT: Tsuneta *et al.*, 1991) aboard *Yohkoh* provides the following characteristics: Most are associated with small flares at their footpoints (Shimojo *et al.*, 1996), lengths lie in the range of a few times $10^4 - 4 \times 10^5$ km, widths $1 - 4 \times 10^4$ km, apparent velocities from $150 - 800$ km s^{-1} with an average velocity of about 200 km s^{-1}. Their lifetimes may extend to several hours with a power law distribution with an index of ~ 1.2 (Shimojo *et al.*, 1996). A large percentage (76 %) of the jets show constant or converging shapes; the width of the jet is constant or decreases with distance from the footpoint. While X-ray jets seem to have well-studied lifetimes, lengths, thicknesses and speeds (Shimojo *et al.*, 1996; Cirtain *et al.*, 2007), there is still much work to be done to reveal the relationship between X-ray and EUV jets (Cirtain *et al.*, 2007; Savcheva *et al.*, 2007).

A possible triggering mechanism for solar jets is magnetic reconnection between an emerging magnetic dipolar field and pre-existing solar magnetic field (Yokoyama and Shibata, 1995; Canfield, Pevtsov, and McClymont, 1996). Magnetic reconnection is a fundamental process in astrophysical plasmas wherein magnetic fieldlines from different magnetic flux systems that come into contact, change their connectivity and eventually convert their free magnetic energy into kinetic and thermal energy of the plasma (Priest and Démoulin, 1995). Reconnection under solar coronal conditions is an energetic event; for the field strengths, densities and speeds involved in the interaction between emerging flux systems and ambient fields, reconnection can trigger the launch of high-speed (hundreds of $\mathrm{km\,s^{-1}}$), high-temperature (10^7 K) plasma jets (Galsgaard *et al.*, 2005; Gontikakis, Archontis, and Tsinganos, 2009; Moreno-Insertis, 2009). Observations have revealed the recurrent emission of jets (*e.g.*, Chifor *et al.*, 2008). Moreover, numerical models have reported on the recurrent emission of jets after flux emergence in the vicinity of small active regions (Archontis, Tsinganos, and Gontikakis, 2010) or when photospheric stress is constantly applied within a unipolar region (Pariat, Antiochos, and DeVore, 2010). In addition, observations and simulations (Del Zanna, 2008; Török *et al.*, 2009; Harra *et al.*, 2012) have shown the existence of persistent (hot and cool) outflows adopting jet-like characteristics around active regions. These outflows are likely to occur as a byproduct of the compression of the magnetic fields during reconnection. It is worthwhile mentioning that numerical experiments (*e.g.* Nishizuka *et al.*, 2008; Moreno-Insertis, 2009; Harra *et al.*, 2012) have successfully reproduced the simultaneous emission of hot and cool plasma along jets, a feature supported by recent solar missions.

Shen *et al.* (2011) showed that the non-potential magnetic field of the jet is enough to supply the total energy for the jet and that the twist of the closed field indeed affects the flux tubes stability. The authors observed three distinct phases in the radial expansion of the jet and proposed that since the jet is driven by magnetic twist through the reconnection process, each of these phases, the rising, radially expanding, and unwinding phase of the jet, is a different manifestation of the reconnection.

Chen, Zhang, and Ma (2012) present a detailed study of a jet which showed a distinct transverse rotating motion during its ejection. The observational results appear to be consistent with an untwisting model of magnetic reconnection (*e.g.*, Shibata and Uchida, 1986; Pariat, Antiochos, and DeVore, 2010). By tracking six identified features moving helically in the jet, they found that the jet plasma moved at an approximately constant velocity along the axial direction and made a circular motion in the plane perpendicular to the jet axis. The authors derived the mean values of the axial velocity (114 $\mathrm{km\,s^{-1}}$), transverse velocity (136 $\mathrm{km\,s^{-1}}$), angular speed ($0.81^\circ\,\mathrm{s^{-1}}$), rotation period (452 s) and rotation radius (9.8×10^3 km) for each moving feature. Most of these results were similar to the results by Shen *et al.* (2011).

Hinode observations of polar coronal holes reveal that X-ray jets have two distinct velocities: one near the Alfvén speed (800 $\mathrm{km\,s^{-1}}$) and another near the sound speed (200 $\mathrm{km\,s^{-1}}$). Cirtain *et al.* (2007) fitted the slope in the height–time diagrams of the intensity front of four jets to derive the velocity of the outflowing plasma. The authors observed multiple velocity components for each jet. One component is consistent with the above-mentioned spatiotemporal average velocity of ~ 200 $\mathrm{km\,s^{-1}}$, while another much faster (~ 800 $\mathrm{km\,s^{-1}}$) component is observed at the start of each event and according to the authors it constitutes evidence for material being ejected during relaxation of the magnetic field after reconnection. They also found that this high-speed mass flow sometimes occurs multiple times per jet; presumably there is an Alfvén wave generated during each burst of reconnection (Liu *et al.*, 2009).

Liu *et al.* (2009) studied a chromospheric jet and reported that the ejection occurred in three episodes separated by 12 – 14 minutes, rather than continuously. The amount and velocity of ejected material decreased with time. The acceleration inferred from parabolic tracks in the time-distance diagram had a mean of 141 $\mathrm{m\,s^{-2}}$, a fraction of the solar gravitational acceleration. Feng *et al.* (2012) reported, based on the analysis of 27 jets by Wang *et al.* (1998), that in all cases the velocity of the centroid was much less than the velocity of the leading edge, indicating that the jets stretch out rapidly as they propagate through the corona.

In this paper we study coronal jets using high cadence 304 Å images from the *Atmospheric Imaging Assembly* (AIA: Lemen *et al.*, 2012) aboard the *Solar Dynamics Observatory* (SDO: Pesnell, Thompson, and Chamberlin, 2012). The sample consists of four jets on 25 June 2010, two of which are close to the equator, and two jets on 30 June 2010. Our aim is to study the evolution and basic physical properties of these jets. All events evolve in a rather short time scale and reach large heights above the photosphere, although their maximum height, speed, acceleration and magnetic topology differ in each case. The high-resolution observations reveal that some jets have an overall twisted configuration. From this element we argue that magnetic mechanisms may play a significant role in the triggering and evolution of these jets.

2. Methodology and Data Analysis

For our analysis, we measure the *leading edge* of the jet as a function of time in each jet and construct height–time diagrams. We visually define the leading edge as the highest endpoint of the jet over the 304 Å background, *i.e.* the point where the brightening extension stops. Savcheva *et al.* (2007) have reported on four different methods for the determination of the apparent outward velocity of the jets. Since all our jets are quite bright, we do not have to resort to advanced image processing methods to uncover the leading edge. In many respects, our method is similar to the extraction of height–time diagrams from white light coronagraph images of CMEs. These diagrams allow us to follow the evolution of the plasma ejection in the solar gravitational field and estimate useful physical parameters, such as the initial jet speed of the leading edge and its mean acceleration by assuming an upwards ballistic motion of the plasma. Since we analyze a single wavelength, we cannot say whether the jet terminates at the measured height or its plasma moves out of the 304 Å passband (*i.e.*, due to heating) or it becomes too faint due to density decrease as it extends further out in the corona (Savcheva *et al.*, 2007). So our results refer solely to the motion of the cool component of the jet plasma.

The data processing is relatively straightforward. We have obtained detailed height–time diagrams of the solar jets (Figure 1) using the synoptic, level-1.5 medium cadence (90 sec) observations in the AIA 304 Å channel. Our data are images in Flexible Image Transport System (FITS) format binned to 1024×1024 pixels. We obtain the heliographic coordinates of the leading edge of the jet in every frame using the routines FITSHEAD2WCS and WCS_GET_COORD. We then calculate the projected height from the solar surface. Because all of our jets are very close to the limb (Figure 2), projection effects are minimized and the projected height should be close to the actual radial height. Nevertheless, we plan a future comparison of the present observations with those of STEREO/SECCHI which should provide the three-dimensional (3D) quantities, albeit at a slightly lower temporal resolution (5 min).

One possibility for the motion of the jet plasma is that it undergoes a ballistic motion. To investigate this possibility, we fit the height–time data with a quadratic equation to extract the kinematics of the jets' leading edges:

$$h(t) - h(t_0) = u_0 t - \frac{1}{2} a_0 t^2 \tag{1}$$

which more specifically provides the *initial* speed, u_0 and acceleration, a_0 of the jet, t_0 is defined as the moment in which the event begins to eject and $h(t_0)$ the height in the corresponding time frame. To calculate error bars, we use the maximum error in visually locating the leading edge. We estimate this error to about three pixels in either the x-axis or y-axis. In Section 4, we shall subtract from a_0 the solar acceleration of gravity g to isolate the upwards accelerating forces. Thus, we may estimate, for example, the part which is due to the higher plasma pressure at the base of the jet as compared to the pressure at larger heights. This simple argument may give clues as to the nature of the driving mechanism of the jets.

3. Physical Characteristics of Jets

In this section the data for each of the jets of the present study are analyzed and briefly discussed. We have followed the evolution of the regions, from where the jets are emitted for two hours. We summarize the characteristics of these jets in Table 1. It is worthwhile mentioning that we have not found evidence of other jet-like emission in the same locations, apart from the events reported in Table 1. However, we note that the jet on 30 June has an earlier jetting episode at the same location while the two jets in the southern coronal hole (SCH), on 25 June, originate very close to each other but at different times. These events suggest recurrent emission at those locations. However, we chose to treat them as separate events. Our analysis (see Table 1) indicates that the "precursor" jets emitted first tend to reach lower heights, occur over a shorter time period and have lower speeds than the latter jets. In this very strict sense and for simplicity, we use the terms "precursor" and "main" to label the two successive jets, respectively.

Table 1 summarizes the results of the analysis for the jets observed by AIA on 25 June 2010 and the jet of 30 June 2010 obtained by the polynomial fitting of their leading edge motion. Specifically, we present the initial velocity (u_0) and the acceleration (a_0) of the ballistic fitting, the maximum height (h_{max}), the lifetime, the gravitational acceleration that corresponds at each maximum height ($g(h_{\mathrm{max}})$), the initial triggering time (t_0) and the inclination angle (ϕ) of each event.

Figure 1a and Figure 2a correspond to a North-West quiet Sun jet occurring very close to the limb. From the height–time diagram, the jet reaches a maximum height $\sim 0.19 R_{\odot}$, *i.e.*, $\sim 132\,000$ km. The duration of the jet is ~ 37 min. No apparent helical structure is

Table 1 Characteristics of the plasma jets

	u_0 [km s^{-1}]	a_0 [km s^{-2}]	h_{max} [% $R_{\odot}$]	Lifetime [min]	$g(h_{\mathrm{max}})$ [km s^{-2}]	t_0 [UT]	ϕ
25 June 2010							
North-West (NW) Jet	760	0.16	19	37.4	0.19	19:54:02	45°
South-West (SW) Jet	94	0.03	9	46.6	0.23	19:24:02	30°
South Coronal Hole (SCH) First Jet	150	0.21	9	21.0	0.23	18:58:38	30°
SCH Second Jet	440	0.09	11	39.0	0.22	20:03:02	40°
30 June 2010							
Main Jet	250	0.17	27	43.4	0.17	03:26:15	15°
'Precursor'	155	0.13	15	34.6	0.21	03:00:02	5°

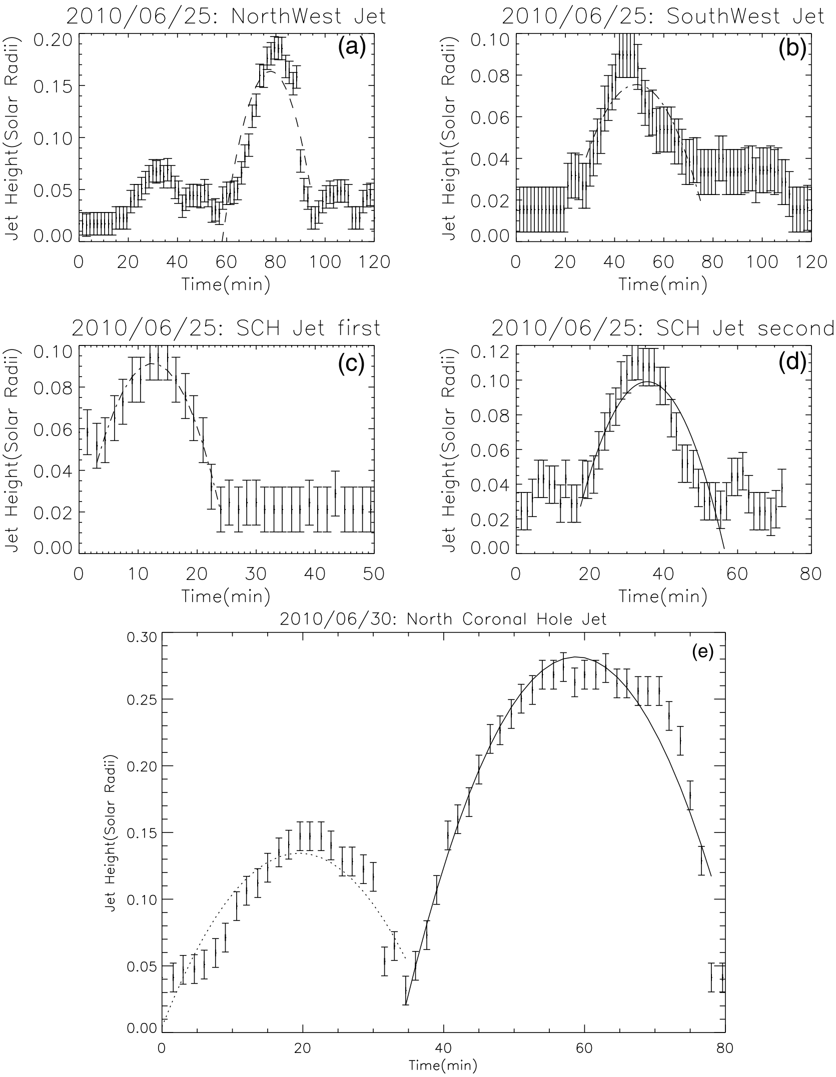

Figure 1 Height–time diagrams for the jets observed by AIA in 304 Å (bars). The dashed and dot–dashed curves correspond to the polynomial interpolation of the 304 Å observations. (a) North-West Jet. (b) South-West Jet. (c) South Coronal Hole first jet. (d) The line shows the corresponding polynomial interpolation of the second jet, which occurs at the same extended emission area of the South Coronal Hole. (e) Height–time diagram of the 2010/06/30 jet and its "precursor" using AIA 304 Å observations. The solid (dotted) lines represent the polynomial fits of the main ("precursor") jet, respectively.

observed. This jet has the largest inclination in our sample, which is about a 45° North–South inclination. For this reason, in our analysis we took into account the vertical distance of the leading edge of the jet from the Sun. With the escape speed from the Sun about 618 $\mathrm{km\,s^{-1}}$ at photospheric levels ($\sim$360 $\mathrm{km\,s^{-1}}$ at $1.7R_{\odot}$), the initial speed seems sufficient for the plasma to overcome solar gravity and escape into interplanetary space, if the plasma of the jet were ejected radially outwards in a vacuum.

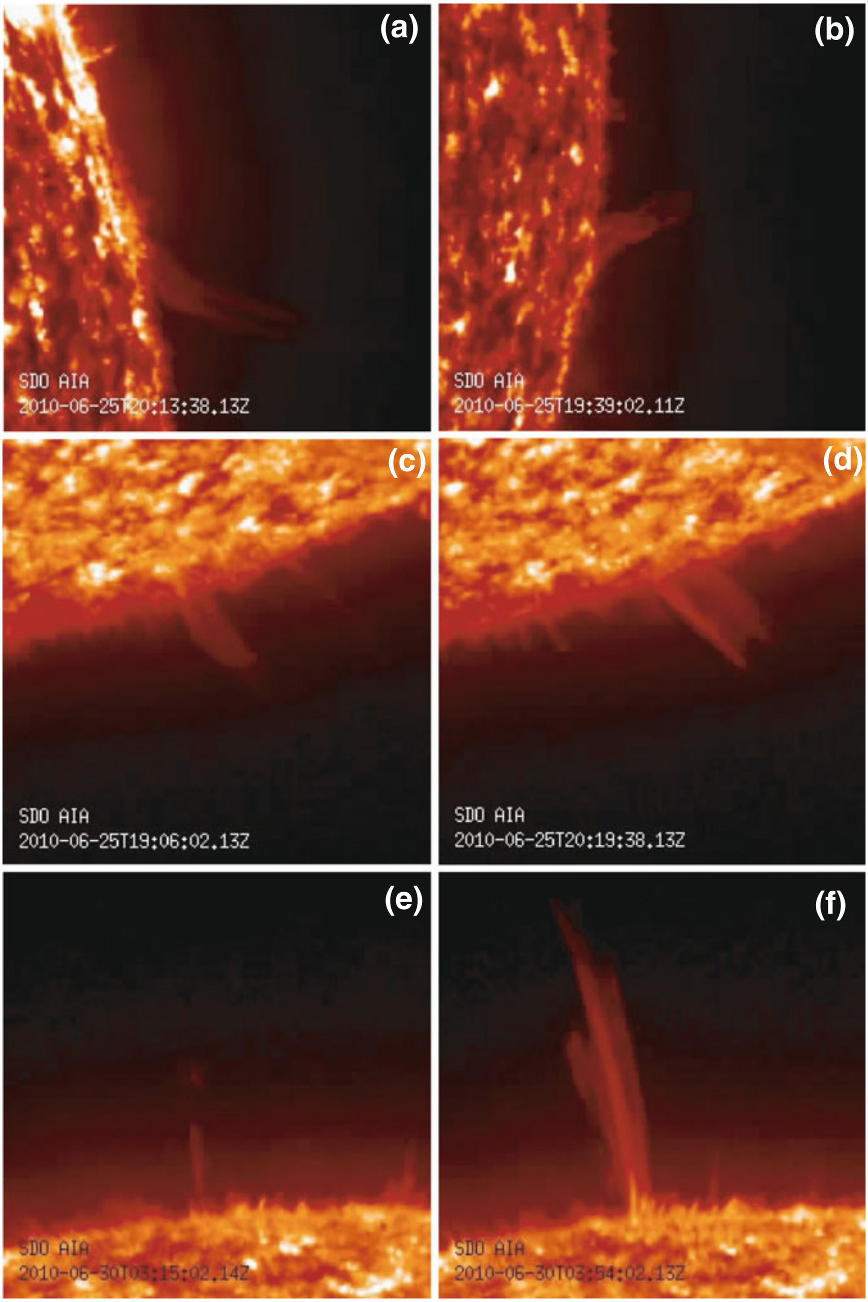

Figure 2 AIA 304 Å snapshots of the jets analyzed in this paper. (a) North-West Jet, (b) South-West Jet, (c, d) "precursor" and "main" Southern Coronal Hole jets, (e, f) "precursor" and "main" Northern Coronal Hole jets. The snapshots were taken at the approximate maximum extent of the jet. The times are shown on the figures.

Figure 1b and Figure 2b correspond to a South-West quiet Sun jet. The position of this jet is close to the solar limb, and thus, it is quite convenient to analyze its structure and behavior. The online movie of the AIA 304 Å observations reveals a clear helical configuration and an untwisting motion of the jet plasma. From the height–time diagram, we find that the jet reaches a maximum height of $\sim 0.09 R_{\odot} \sim 63\,000$ km and lasts for ~ 47 min (Table 1). In this case, the initial speed of the jet is too low for the plasma to overcome solar gravity and escape in interplanetary space.

Figure 1c and Figure 2c correspond to the first jet that occurs at the south pole (first SCH jet). The jet reaches a maximum height of $\sim 0.09 R_{\odot}$ and lasts for ~ 21 min. In addition, there is another jet at the same extended emission area (second SCH jet) reaching a height of $\sim 0.11 R_{\odot}$ and lasting for ~ 39 min. These two jets also show a helical structure (see online movies[1]).

The 30 June 2010 event appearing at the northern solar pole is a much longer jet than those occurring on June 25 (Figure 2e, f). It reaches a maximum height of $\sim 0.27 R_{\odot}$ ($\sim 190\,000$ km) and lasts for 44 min (Figure 1 bottom panel). Untwisting motions are evident (see online movie) and they again imply a helical configuration for the jet. As can be seen in the movie and in the bottom panel of Figure 1, this jet is recurrent. The "precursor" reaches a smaller height of $\sim 0.15 R_{\odot}$ and lasts for ~ 35 min. It is much slower and narrower than the main jet (Table 1), but it has almost the same speed as the SCH first jet on 25 June (Table 1). Despite its striking 304 Å signature, the speeds of both the main jet and its "precursor" are much lower than the solar escape speed. The magnitude of the solar gravitational acceleration ($g = 0.274$ km s^{-2}) exceeds the derived deceleration of the jet and its "precursor". This is an indication that gravitational forces are not the only ones acting on the jet plasma but there are instead other opposing forces, such as electromagnetic forces, pressure gradients, *etc.*, which apparently contribute to the upward motion of the rising plasma of the jet, as we discuss in the following section.

4. Two Components of the Acceleration of the Jets

Previous work by Feng *et al.* (2012) showed that the kinematic trajectories of solar jets could be fitted successfully with a ballistic model (Wood *et al.*, 1999). Moreover, in some cases (Ko *et al.*, 2005), such a ballistic model could also explain several dynamical properties of a jet. In their model it was assumed that the gas was ejected upward from the surface with a range of initial speeds. The smooth change of the upflow-to-downflow speed at a certain altitude derived from the ballistic model was found to be consistent with the change of the line intensities from Doppler dimming observed by UVCS/SOHO. On the other hand, Patsourakos *et al.* (2008) reported on a jet that had kinematically two discrete phases: one slow rise phase followed by a "jump" and *rapid, impulsive acceleration* to a fraction of the Alfvén speed. Their results are consistent with a twist model (Pariat, Antiochos, and DeVore, 2009), in which the jet is driven by magnetic untwisting, and predict the development of a clear helical structure. In this simulation, a vertically oriented magnetic dipole, embedded below the photosphere, generates a null point in the corona which also contains a uniform-background vertical magnetic field. The resulting axisymmetric configuration contains two distinct flux

[1] https://www.dropbox.com/s/oiqr3kgqzzpd7gj/100625_nw.mov,
https://www.dropbox.com/s/e2vgg3c0eorw92m/100625_sw.mov,
https://www.dropbox.com/s/u91yaaugmh5ksib/100625_sch.mov,
https://www.dropbox.com/s/c33eqqll3bzlmz0/100630_nch.mov.

systems: a circular patch of strong closed magnetic flux surrounded by weaker open flux, leading to an axisymmetric configuration. In the following, we attempt to elaborate whether the assumption of a ballistic motion is appropriate to describe the plasma motion of the jet, and estimate the upward non-gravitational forces acting along the jet.

First, in the ballistic model we have assumed that the total deceleration which the leading edge of the jet experiences along its motion is constant. We denoted the magnitude of this constant deceleration by a_0. If the value of a_0 is everywhere less than the magnitude of the downwards solar gravitational acceleration, $g_{\odot}(r) = GM/r^2$, there must exist some upward acceleration of the leading edge of the jet. We denote this upward plasma acceleration by $f_0^{\mathrm{up}}(r)$, *i.e.*

$$a_0 = g_{\odot}(r) - f_0^{\mathrm{up}}(r), \qquad f_0^{\mathrm{up}}(r) = g_{\odot}(r) - a_0. \tag{2}$$

If the ballistic assumption $a_0 = \text{const.}$ were correct, $f_0^{\mathrm{up}}(r)$ would give the upward forces (per unit mass) acting on the jet, while in a pure ballistic motion without non-gravitational forces $f_0^{\mathrm{up}}(r)$ would be null. Figure 3 gives plots of $f_0^{\mathrm{up}}(r)$ for the jets. In all cases we see that $f_0^{\mathrm{up}}(r) > 0$, which means that during the upward motion of the plasma there exist non-gravitational forces which weaken the effect of $g_{\odot}(r)$.

On the other hand, we may calculate these non-gravitational forces without assuming a ballistic motion. From our height–time diagrams the first derivative of the height $h(t)$ of the leading edge of the jet gives the dynamical velocity of the event $u(t)$. And, the second height derivative of $h(t)$ indicates the dynamical deceleration of the leading edge of the jet. We denote the magnitude of this nonconstant deceleration by $a_1(t)$. If the value of $a_1(t)$ is everywhere less than the magnitude of the downwards solar gravitational acceleration, $g(h(t))$, there must exist some upwards acceleration of the leading edge of the jet. We denote this upward plasma acceleration by $f_1^{\mathrm{up}}(r)$, *i.e.*,

$$a_1 = g\bigl(h(t)\bigr) - f_1^{\mathrm{up}}(r), \qquad f_1^{\mathrm{up}}(r) = g\bigl(h(t)\bigr) - a_1. \tag{3}$$

Each instantaneous acceleration value corresponds to a specific height and moment in the evolution of the event in each jet. We also calculate the solar gravitational acceleration in each corresponding height $g(h(t))$. The acceleration $f_1^{\mathrm{up}}(r)$ gives the upward forces (per unit mass) acting on the jet. Figure 3 shows plots of $f_1^{\mathrm{up}}(r)$ for the observed jets. Similarly with the previous case of the ballistic assumption, in all cases we see that $f_1^{\mathrm{up}}(r) > 0$, which means that during the upward motion of the plasma there exist non-gravitational forces which weaken the effect of $g_{\odot}(r)$.

The plots in Figure 3 indicate that in every case $f_1^{\mathrm{up}}(r) > f_0^{\mathrm{up}}(r) > 0$, *i.e.*, $f_1^{\mathrm{up}}(r) > 0$ which takes into account the dynamical evolution of the plasma's acceleration, is larger than $f_0^{\mathrm{up}}(r) > 0$, which is based on the assumption that acceleration is constant throughout the whole jets' lifetime. This indicates that $a_1(t)$ is of lower value than the constant value a_0 of the ballistic model throughout the occurrence of the jets.

5. Discussion and Conclusions

The analysis of the observations of the sample of the jets revealed a relatively wide range of temporal evolution ($\sim 20 - 50$ min) during which these explosive events are triggered and evolved. Their initial speeds ranged from less than 100 km s^{-1} to more than 700 km s^{-1} with accelerations between 30 and 210 m s^{-2}. The jets reach a maximum height from ~ 10 % of the solar radius, to ~ 30 % of the solar radius for the larger events. The initial speeds are less than the escape speed from the Sun at the given height, with the exception of the North-West

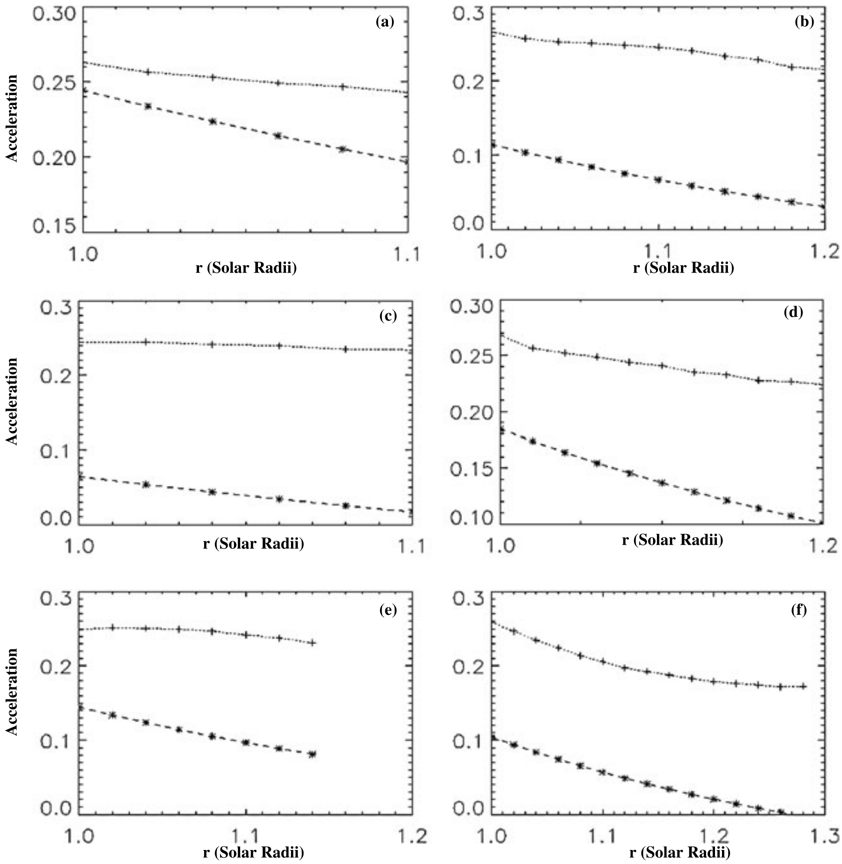

Figure 3 The acceleration profile $f_0^{\mathrm{up}}(r)$ and dynamical acceleration profile $f_1^{\mathrm{up}}(r)$ of the leading edge of the analyzed jets, due to forces other than solar gravity *vs.* distance in solar radii ($1.00R_\odot$ is at the photospheric level). North-West Jet (a), South-West Jet (b), "precursor" and "main" South Coronal Hole (c and d, respectively), "precursor" and "main" Northern Coronal Hole jets (e and f, respectively). In every panel the '*' correspond to each jet's $f_0^{\mathrm{up}}(r)$ and the "+" correspond to each jet's $f_1^{\mathrm{up}}(r)$.

Jet on 25 June 2010. It is worthwhile to mention that in the present study we only took into account the speed of the leading edge of the jet. Projection effects (*e.g.* by using STEREO data), other characteristic speeds in the jet motion, such as the jet centroid speed, the initial speed of the centroid, *etc.* (*e.g.* Feng *et al.*, 2012) are beyond the scope of this preliminary analysis of the basic characteristics of a sample of recent SDO jets and will be taken into account in another study.

With regards to the deceleration of the jets, we found that the magnitude of the downward solar gravity is weaken by upwards opposing accelerating forces in any jet or its "precursor", for all the events presented in our study. This fact indicates clearly that there are also other opposing forces acting on the jet plasma than gravity. Nevertheless, in all cases, we find that the gravitational forces dominate and the net result is a decelerating upward motion of the plasma in the jets.

In two of our cases we have indications of recurrency at the same location or source region (Figure 1 bottom, Figure 2) and untwisting suggestive of a helical magnetic field configuration. Further investigation is required to reveal the triggering mechanism(s) that leads to the onset of these jets and affects their subsequent evolution.

Since the jets presented in this paper reveal some differences in their properties and characteristics (*e.g.* possibly recurrent behavior, helical structure, speed magnitude) it is possible that various physical processes may contribute to their triggering. One possible mechanism is magnetic reconnection. The magnetic tension of the reconnected fieldlines can lead to the acceleration of high-speed jets. The atmospheric height where reconnection occurs is important, as it might determine the temperature of the plasma which will be emitted. The existence of cool and hot material in the jets could be the result of parallel reconnection events, at small and large atmospheric heights, respectively (*e.g.* Nishizuka *et al.*, 2008).

On the other hand, temperature and density enhancements could also be produced by adiabatic compression and then, high velocity outflows (jets) can be formed via pressure increase when there are horizontal converging flows toward the site of emission. For instance, interacting magnetic flux systems that consist *e.g.* of field lines pointing in parallel directions (and therefore have limited efficiency to reconnect) can build up strong pressure gradients at their interface. The corresponding pressure gradient force can lift up dense plasma against gravity and lead to the onset of a jet.

We expect that in a highly dynamic 3D environment, such as the solar atmosphere, both processes may be at work. The effect of each mechanism on the physical properties and characteristics of the produced jets requires further investigation and it will be explored in a forthcoming paper by means of numerical experiments and combined high-resolution observations.

We also studied whether the jets undergo a ballistic motion during their evolution. Firstly, we calculated the non-gravitational acceleration of the jet ($f_0^{\mathrm{up}}(r)$), assuming a ballistic model and then we repeated the calculation ($f_1^{\mathrm{up}}(r)$) for a simplified dynamical (non-ballistic) model. These upward plasma accelerations could be due, say, to a higher plasma pressure at the base of the jet as compared to the pressure at larger heights r, or upward-directed magnetic forces. In turn, the higher pressure at the base of the jets could be due to energy release by magnetic reconnection, or due to an increased base temperature before the jet takes off.

In the ballistic model, there is a pronounced decrease of the acceleration with distance from the solar surface. In the dynamical model approximation, the acceleration varies less with height and in some cases (*e.g.* see panels a, c, e in Figure 3) this drop is small. This is an interesting result, which indicates that an almost constant force drives the upward motion of the jet during its evolution. Moreover, comparing the magnitude of the accelerations obtained in the two cases, we find that $f_1^{\mathrm{up}}(r)$ is larger than $f_0^{\mathrm{up}}(r)$ for all jets. Therefore, it is revealed that the ballistic approximation is not in satisfactory agreement with the dynamical evolution of the leading edge of the jets.

Acknowledgements We thank the referee for the useful comments, which have improved the manuscript. SDO is a mission of NASA's Living With a Star Program. A.V. is supported by NASA contract S-136361-Y. S.P.M. acknowledges financial support by the Alexander Onassis Public Benefit Foundation and also the Foundation for Education and European Culture (IPEP) in Greece. The work presented here is supported by the Hellenic National Network for Space Research (HNSR), MIS 377274 (Thalis).

References

Archontis, V., Tsinganos, K., Gontikakis, C.: 2010, *Astron. Astrophys.* **512**, L2.

Beckers, J.M.: 1972, *Annu. Rev. Astron. Astrophys.* **10**, 73.
Canfield, R.C., Pevtsov, A.A., McClymont, A.N.: 1996, *Astron. Soc. Pac. Conf. Ser.* **111**, 341.
Chen, H.-D., Zhang, J., Ma, S.-L.: 2012, *Res. Astron. Astrophys.* **12**, 573.
Chifor, C., Isobe, H., Mason, H.E., Hannah, I.G., Young, P.R., Del Zanna, G., Krucker, S., Ichimoto, K., Katsukawa, Y., Yokoyama, T.: 2008, *Astron. Astrophys.* **491**, 279.
Cirtain, J.W., Golub, L., Lundquist, L., van Ballegooijen, A., Savcheva, A., Shimojo, M., DeLuca, E., Tsuneta, S., Sakao, T., Reeves, K., Weber, M., Kano, R., Narukage, N., Shibasaki, K.: 2007, *Science* **318**, 5856. 1580.
Del Zanna, G.: 2008, *Astron. Astrophys.* **481**, L49.
Feng, L., Inhester, B., de Patoul, J., Wiegelmann, T., Gan, W.Q.: 2012, *Astron. Astrophys.* **538**, 9.
Filippov, B., Golub, L., Koutchmy, S.: 2009, *Solar Phys.* **254**, 259.
Galsgaard, K., Moreno-Insertis, F., Archontis, V., Hood, A.: 2005, *Astrophys. J. Lett.* **618**, L153.
Gontikakis, C., Archontis, V., Tsinganos, K.: 2009, *Solar Phys.* **506**, L45.
Harra, L.K., Archontis, V., Pedram, E., Hood, A.W., Shelton, D.L., van Driel-Gesztelyi, L.: 2012, *Solar Phys.* **278**, 47.
Kamio, S., Hara, H., Watanabe, T., Matsuzaki, K., Shibata, K., Culhane, L., Warren, H.P.: 2007, *Publ. Astron. Soc. Japan* **59**, S757.
Ko, Y.K., Raymond, J.C., Gibson, S.E., Alexander, D., Strachan, L., Holzer, T., Gilbert, H., St. Cyr, O.C., Thompson, B.J., Pike, C.D., Mason, H.E., Burkepile, J., Thompson, W., Fletcher, L.: 2005, *Astrophys. J.* **623**, 519.
Lemen, J.R., Title, A.M., Akin, D.J., Boerner, P.F., Chou, C., Drake, J.F., Duncan, D.W., Edwards, C.G., Friedlaender, F.M., Heyman, G.F., Hurlburt, N.E., Katz, N.L., Kushner, G.D., Levay, M., Lindgren, R.W., Mathur, D.P., McFeaters, E.L., Mitchell, S., Rehse, R.A., Schrijver, C.J., Springer, L.A., Stern, R.A., Tarbell, T.D., Wuelser, J.-P., Wolfson, C.J., Yanari, C., Bookbinder, J.A., Cheimets, P.N., Caldwell, D., Deluca, E.E., Gates, R., Golub, L., Park, S., Podgorski, W.A., Bush, R.I., Scherrer, P.H., Gummin, M.A., Smith, P., Auker, G., Jerram, P., Pool, P., Soufli, R., Windt, D.L., Beardsley, S., Clapp, M., Lang, J., Waltham, N.: 2012, *Solar Phys.* **275**, 17.
Liu, W., Berger, T.E., Title, A.M., Tarbell, T.D.: 2009, *Astrophys. J. Lett.* **707**(1), L37.
Liu, W., Berger, T.E., Title, A.M., Tarbell, T.D.: 2011, *Astrophys. J.* **728**(2), 103.
Massi, M., Poletto, G.: 2011, *Mem. Soc. Astron. Ital.* **82**, 145.
Moreno-Insertis, F.: 2009, *IAU Symp.* **259**, 201.
Nishizuka, N., Shimizu, M., Nakamura, T., Otsuji, K., Okamoto, T., Shibata, K., Katsukawa, Y.: 2008, *Astrophys. J. Lett.* **683**, L83.
Nisticó, G., Bothmer, V., Patsourakos, S., Zimbardo, G.: 2009, *Solar Phys.* **259**, 87.
Pariat, E., Antiochos, S.K., DeVore, C.R.: 2009, *Astrophys. J.* **691**, 61.
Pariat, E., Antiochos, S.K., DeVore, C.R.: 2010, *Astrophys. J.* **714**, 1762.
Patsourakos, S., Pariat, E., Vourlidas, A., Antiochos, S.K., Wuelser, J.P.: 2008, *Astrophys. J. Lett.* **680**, L73.
Pesnell, W.D., Thompson, B.J., Chamberlin, P.C.: 2012, *Solar Phys.* **275**, 3–15. doi:10.1007/s11207-011-9841-3.
Priest, E.R., Démoulin, P.: 1995, *J. Geophys. Res.* **100**(A12), 23443.
Roy, J.R.: 1973, *Solar Phys.* **28**, 95.
Savcheva, A., Cirtain, J., Deluca, E., Lundquist, L., Golub, L., Weber, M., Shimojo, M., Shibasaki, K., Sakao, T., Narukage, N., Tsuneta, S., Kano, R.: 2007, *Publ. Astron. Soc. Japan* **59**, S771.
Shen, Y., Liu, Y., Su, J., Ibrahim, A.: 2011, *Astrophys. J. Lett.* **735**, L43.
Shibata, K., Uchida, Y.: 1986, *Solar Phys.* **103**, 299.
Shibata, K., Nakamura, T., Matsumoto, T., Otsuji, K., Okamoto, T.J., Nishizuka, N., Kawate, T., Watanabe, H., Nagata, S., UeNo, S., Kitai, R., Nozawa, S., Tsuneta, S., Suematsu, Y., Ichimoto, K., Shimizu, T., Katsukawa, Y., Tarbell, T.D., Berger, T.E., Lites, B.W., Shine, R.A., Title, A.M.: 2007, *Science* **318**, 1591.
Shimojo, M., Hashimoto, S., Shibata, K., Hirayama, T., Hudson, H.S., Acton, L.W.: 1996, *Publ. Astron. Soc. Japan* **48**, 123.
Török, T., Aulanier, G., Schmieder, B., Reeves, K.K., Golub, L.: 2009, *Astrophys. J.* **704**, 485.
Tsinganos, K., Ray, T., Stute, M.: 2009, *Protostellar Jets in Context*, *Astrophysics and Space Science Proceedings Series*. Springer, Berlin.
Tsuneta, S., Acton, L., Bruner, M., Lemen, J., Brown, W., Caravalho, R., Catura, R., Freeland, S., Jurcevich, B., Owens, J.: 1991, *Solar Phys.* **136**, 37.
Tziotziou, K., Tsiropoula, G., Sütterlin, P.: 2005, *Astron. Astrophys.* **444**, 265.
Wang, Y.M., Sheeley, N.R. Jr., Socker, D.G., Howard, R.A., Brueckner, G.E., Michels, D.J., Moses, D., St. Cyr, O.C., Llebaria, A., Delaboudiniére, J.P.: 1998, *Astrophys. J.* **508**, 899.
Wood, B.E., Karovska, M., Cook, J.W., Howard, R.A., Brueckner, G.E.: 1999, *Astrophys. J.* **523**, 444.
Yokoyama, T., Shibata, K.: 1995, *Nature* **375**, 6526, 42.